Published in final edited form as:
Biochem Biophys Res Commun. 2008 August 1; 372(3): 412–417. doi:10.1016/j.bbrc.2008.05.053.

Epithelial V-like Antigen Regulates Permeability of the Blood-CSF Barrier

Gouri Chatterjee[a], **Lisette M. Carrithers**[a], and **Michael D. Carrithers**[a,b,*]

a *Department of Neurology, Yale University School of Medicine, New Haven, CT, USA*

b *Program in Human and Translational Immunology, Yale University School of Medicine, New Haven, CT, USA*

Abstract

Epithelial V-like antigen (EVA), a CD3-binding immunoglobulin-like protein, regulates embryonic thymic development. Here we demonstrate that EVA is expressed in choroid plexus from mature immune competent and lymphocyte deficient (RAG−/−) mice. Choroid plexus epithelial cells from RAG−/− mice demonstrated reduced junctional integrity and enhanced permeability that was associated with decreased expression of E-cadherin and EVA mRNA as compared to wild-type mice. Following iv infusion of an anti-CD3 antibody (145-2C11) that also binds EVA, expression of E-cadherin and EVA mRNA approached levels seen in wild type mice. Immuno-fluorescent staining for cadherin also revealed decreased expression in untreated RAG−/− mice that could be increased by 145-2C11 treatment. Expression of mouse EVA in HEK-293 cells followed by challenge with 145-2C11 resulted in increased cytosolic calcium that was not seen in control cells. These results suggest that EVA expressed in choroid plexus cells may regulate the permeability of the blood-CSF barrier.

Keywords

Epithelial V-like antigen; choroid plexus; blood-CSF barrier; cadherin; F-actin; signal transduction; cytosolic calcium

Introduction

T lymphocytes and other immune cells traffic through the neuroprotective barriers continually in the absence of inflammation to protect the host from severe infections. A steady state number of T lymphocytes is maintained within the CNS to perform this immune surveillance [1]. How this steady state is maintained is unclear. Our prior work and that of others demonstrated that immune surveillance of the brain by T lymphocytes occurs primarily through the blood-CSF barrier rather than the blood-endothelial barrier at the blood-brain barrier (BBB) [2–5]. Transmigration of T lymphocytes through the blood-CSF barrier requires binding of the T cell to P-selectin expressed on the choroid plexus epithelium, and the junctional integrity between the epithelial cells forms the blood-CSF barrier [3–5]. Based on these data, we hypothesized

*Corresponding author: Michael D. Carrithers, Department of Neurology, Yale University School of Medicine, PO Box 208018, New Haven, CT 06520-8018, Tel: 203-737-2534, Fax: 203-785-5694, E-mail address: E-mail: michael.carrithers@yale.edu.

that regulation of steady state numbers of CNS T lymphocytes occurs at the level of the blood-CSF barrier through modification of the junctions between choroid plexus epithelial cells.

Here we analyzed the choroid plexus in wild type and lymphocyte deficient mice (RAG−/−). The goal was to determine whether or not the blood-CSF barrier was more permissive in lymphocyte-deficient animals in order to permit enhanced immune surveillance of the CNS and maintain a constant level of T lymphocytes within the CNS. Consistent with this hypothesis, histologic analysis of the choroid plexus epithelium from RAG−/− mice revealed a reduction in the area of junctional contacts between cells that was associated with enhanced permeability and decreased cadherin expression.

In addition, to characterize a potential mechanism to regulate this gating process, we demonstrate differential expression of epithelial V-like antigen (EVA) in choroid plexus from wild type and immune deficient mice. EVA is an immunoglobulin-like adhesion molecule that is important in embryonic thymic development [6–7]. It has structural homology to the subunits of CD3, the T lymphocyte marker, and binds a monoclonal antibody raised against mouse CD3 (145-2C11) [6–7]. Here adminstration of 145-2C11 *in vivo* resulted in normalization of EVA and cadherin expression in RAG−/− mice closer to wild type levels and led to partial restoration of choroid plexus morphology. *In vitro* activation of EVA by 145-2C11 caused calcium mobilization. These results suggest a novel mechanism to regulate the integrity of the blood-CSF barrier.

Materials and methods

Animals

C57BL6/J wild type and RAG-1 deficient mice were purchased from Jackson Laboratories and used at 6–8 weeks of age. All mice were maintained in sterile and pathogen-free conditions. All animal studies were reviewed and approved by the Yale University School of Medicine Institutional Animal Care and Review Committee (IACUC). For *in vivo* treatment with 145-2C11, mice were injected with 50 μg of antibody 24 hrs prior to sacrifice.

Permeability Assays

Evans blue dye (0.1 ml of a 0.5% wt/vol solution in PBS) was injected intravenously into wild type and RAG-1 −/− C57BL6/J mice [8]. One hour later, mice were anesthetized with ketamine/xylazine, and intracardiac perfusion was performed with ice cold PBS. Brains were isolated, the choroid plexus was microdissected, and dye was extracted from choroid plexus samples in formamide (5 μl/mg of tissue) for three days at room temperature. Absorbance at 650 nm was measured to determine dye concentration.

Immunocytochemistry

Brain frozen sections (7 μm) were either stained with hematoxylin or processed for immunocytochemistry according to standard protocols using bovine serum albumin (BSA), goat serum and Triton X-100 as preincubation blockers [9]. Antibodies were diluted in BSA and Triton X-100 solution and added to the sections for 2 hrs. Sections were washed and incubated with secondary antibody for an additional 1 hr. Primary antibodies were rabbit anti-Pan-cadherin (Abcam) and mouse anti-β-tubulin (Invitrogen), and secondary antibodies were Alexa fluorophore conjugated goat antibodies (Invitrogen). Alexa-546 phalloidin was obtained from Invitrogen. Fluorescent images were obtained on a Zeiss Axiovert 200 fluorescent microscope with either a 20x or 40x objective (Zeiss). Quantitative analysis of cadherin staining was performed with Axiovision 4.6.3 Automeasurement.

RT-PCR and real time analysis

Total RNA was isolated from microdissected choroid plexus tissue by guanidine isothyocyanate lysis and solubilization followed by phenol-chloroform extraction. Samples were then cleaned by column purification (Rneasy; Qiagen). Reverse transcription was performed with Superscript II (Gibco). Quantitative PCR was performed using TaqMan primers (FAM-labeled) commercially obtained (Applied Biosystems), and samples were run on a SmartCycler (Cepheid). Samples were normalized to GAPDH Ct values for each experiment. Each experiment was performed at least three times from separate RNA preparations.

Cells and Transfections

HEK-293 cells are maintained in DMEM supplemented with 10% FBS and glutamine. Mouse EVA-1 cDNA was obtained from Origene in the expression vector, pCMV6-Kan/Neo. Transfections into HEK-293 cells were performed using Lipofectamine (Invitrogen).

Calcium Flux Assays

For calcium flux experiments, HEK-293 cells were labeled with 1 μM Fluo-4 for 30 min. at room temperature. Cells were washed three times with HBSS and then analyzed on an LS-50b fluorometer (Perkin Elmer). Excitation was at 494 nm and emission at 516 nm.

Statistics

Comparisons between groups were made using a Students T test (unpaired, unequal variance) with a $P<0.05$ considered statistically significant (Kaleidagraph 4.03, Synergy Software). Data are expressed as ± SEM.

Results

Choroid Plexus in Immune Competent and Lymphocyte Deficient Mice

We reasoned that in the absence of lymphocyte immune surveillance that the blood-CSF barriers would change functionally to enhance lymphocyte entry. Examination of cellular morphology by hematoxylin staining in C57BL6/J wild type and RAG−/− mice demonstrated that the choroid plexus epithelia from RAG deficient mice were less ordered (Fig. 1AB). There also was less direct contact between cells in the epithelial layer. In other words, the amount of surface area within junctional complexes between cells appeared to be reduced in RAG−/− mice. This result suggested that the epithelial barrier was less tight. In addition, there was no evidence of meningitis or a mononuclear cell infiltration within the choroid plexus or meningeal space in the lymphocyte deficient animals.

To confirm this observation, we measured permeability of microdissected choroid plexus using the Evans Blue technique. As shown in Figure 1C, there was significantly greater leakage of Evans Blue dye into the choroid plexus structure in RAG−/− mice as compared to wild type. The amount of dye leakage normalized to tissue weight was approximately nine-fold greater in RAG−/− choroid plexus; OD650 was 0.009 ± 0.0015 for RAG−/− and 0.001 ± 0.0004 for wild type (n=5; $P=0.004$). Since the capillaries within the choroid plexus are fenestrated and do not provide a blood-endothelial barrier, this leakage reflects the relative integrity of the blood-CSF barrier at the choroid plexus epithelial junctions.

Differential Expression of EVA and E-cadherin in choroid plexus from RAG−/− and wild type mice

To identify potentially novel adhesion molecules in the choroid plexus that could mediate regulation of the blood-CSF barrier, we previously performed microarray analysis of

microdissected choroid plexus from RAG−/− and wild type mice as part of the NIH Neuroscience Microarray Consortium [10]. By this technique (mouse Affymetrix platform), we identified EVA and E-cadherin as being differentially expressed and EVA as a potentially novel regulatory adhesion molecule. Interestingly, as compared to a prior study of EVA in immune deficient mice, EVA expression was reduced in RAG−/− as compared to wild type mice [6]. The opposite expression pattern was observed in the thymus in the prior study.

To confirm this prior observation, we performed real time PCR analysis of mRNA expression for EVA and E-cadherin from choroid plexus. As shown in Table 1, there was approximately 4–8 fold increased expression (2–3 cycle difference by Ct score) of choroid plexus EVA and E-cadherin in samples from wild type mice as compared to RAG−/−. Expression of EVA and E-cadherin increased 2–4 fold (1–2 cycle difference by Ct score) in RAG−/− mice 24 hrs. following infusion of the monoclonal antibody 145-2C11, which binds both CD3 and EVA *in vivo* [6].

To correlate these results with protein expression, we also used immunofluorescence to characterize the morphology of choroid plexus from wild type and RAG−/− mice. As shown in Fig. 2, staining with a pan-cadherin antibody demonstrated reduced expression in lymphocyte deficient RAG−/− mice as compared to wild type mice. In addition, wild type choroid plexus epithelia showed a tightly ordered beaded appearance. RAG−/− choroid plexus epithelial cells appeared more elongated and somewhat atrophic. Although overall staining for β-tubulin was similar between the two conditions, we observed an altered staining pattern for F-actin by phalloidin staining. There appeared to be decreased amounts of F-actin at intercellular junctions in RAG−/− choroid plexus as compared to wild type. These results further suggest that the choroid plexus alters its junctional and cytoskeletal structure in the absence of immune surveillance.

To determine if 145-2C11 treatment (50 μg iv) could increase cadherin protein expression levels as it did for mRNA expression, we examined choroid plexus from treated (24 hrs. post iv infusion) and untreated RAG−/− mice by immune-fluorescence. As shown in Fig. 3, there was increased cadherin staining in choroid plexus epithlelial cells following 145-2C11 treatment that was confirmed by quantitative analysis of images (Table below images in Fig. 3).

145-2C11 ligation of EVA expressed in HEK-293 cells causes an increase in cytosolic calcium

To characterize a potential mechanism that could link EVA to permeability changes in an epithelial barrier, we examined calcium flux in HEK-293 cells transfected with mouse EVA in response to 145-2C11. Although the requirement for extracellular calcium in the formation of cadherin-associated intercellular junctions is well described [11], increases in intracellular calcium also regulate the formation of adherens junctions through increased expression of E-cadherin and increased recruitment of junctional proteins and F-actin to the junctional region [12–13].

Following stimulation with 145-2C11 (0.5 μg/ml final concentration), HEK-293 cells, transfected with mouse EVA and loaded with the calcium indicator dye Fluo-4, demonstrated a rapid and persistent elevation in intracellular calcium that was not seen in control cells transfected with empty vector (Fig. 4A). This response could be partially inhibited by chelation of extracellular calcium with EGTA; however, this reduction was not statistically significant (Fig. 4B). For the EVA-transfected condition, the $\Delta RFU = 11.2 \pm 2.0$ (n=5), for the untransfected condition $\Delta RFU = 0.5 \pm 1.0$ (n=4) ($\underline{P} = 0.004$ as compared to the transfected condition), and for the transfected condition with EGTA $\Delta RFU = 8.3 \pm 0.67$ (n=3). These results suggest that the increase in cytosolic calcium was due primarily to intracellular store release,

although we cannot rule out flux from the extracellular space through plasma membrane channels as a smaller contribution.

Discussion

These data suggest that EVA is expressed in choroid plexus from mature mice and may regulate the permeability of the blood-CSF barrier. Since our prior work demonstrated that T lymphocyte immune surveillance occurs predominantly through the blood-CSF barrier rather than the more restrictive BBB, we focused on examination of the choroid plexus in immune competent and lymphocyte deficient RAG−/− mice. We initially hypothesized that, as in acute inflammation, the choroid plexus epithelia would compensate by increasing expression of adhesion molecules and chemokines to attract lymphocytes to the CSF space. To our surprise, the changes in morphology and gene expression were distinct from those observed in acute inflammation, and we observed differential expression of E-cadherin and EVA in wild type and RAG−/− mice.

We speculate that EVA mediates junctional integrity of the choroid plexus epithelia through increased cadherin expression and recruitment of junctional proteins to the adherens junction [14]. This mechanism could be initiated by ligation of EVA through homotypic-like interactions with CD3 expressed on T lymphocytes followed by subsequent calcium mobilization and downstream signaling events. Although EVA has homology to other Ig-like adhesion molecules, its function here would suggest an inhibitory role to reduce additional T cell migration. This mechanism would represent a novel pathway to regulate T lymphocyte number in the CNS during normal immune surveillance. It also may be relevant to maintenance of normal CNS surveillance and prevention of viral CNS entry during immune suppressive treatments in autoimmune and neoplastic diseases. The use of some newer biologic treatments for these conditions such as rituximab and natalizumab resulted in the development of progressive multifocal leukoencephalopathy (PML), an opportunistic infection of the brain due to the JC virus [15–19]. Prevention of these opportunistic infections during immune therapy is a long term goal of the present work.

Acknowledgements

This work is supported by the National Institutes of Health, the National Multiple Sclerosis Society, a Dana Foundation award in Clinical Hypotheses in Neuroimmunology, and the Bumpus Foundation (to M.D.C.).

References

1. Brabb T, von Dassow P, Ordonez N, Schnabel B, Duke B, Goverman J. In situ tolerance within the central nervous system as a mechanism for preventing autoimmunity. J Exp Med 2000;192:871–80. [PubMed: 10993917]
2. Hickey W, Hsu B, Kimura H. T-lymphocyte entry into the central nervous system. J Neurosci Res 1991;28:254–60. [PubMed: 2033653]
3. Carrithers M, Visintin I, Kang S, Janeway CJ. Differential adhesion molecule requirements for immune surveillance and inflammatory recruitment. Brain 2000;123(Pt 6):1092–101. [PubMed: 10825349]
4. Carrithers M, Visintin I, Viret C, Janeway CJ. Role of genetic background in P selectin-dependent immune surveillance of the central nervous system. J Neuroimmunol 2002;129:51–7. [PubMed: 12161020]
5. Kivisäkk P, Mahad D, Callahan M, Trebst C, Tucky B, Wei T, Wu L, Baekkevold E, Lassmann H, Staugaitis S, Campbell J, Ransohoff R. Human cerebrospinal fluid central memory CD4+ T cells: evidence for trafficking through choroid plexus and meninges via P-selectin. Proc Natl Acad Sci U S A 2003;100:8389–94. [PubMed: 12829791]
6. Guttinger M, Sutti F, Panigada M, Porcellini S, Merati B, Mariani M, Teesalu T, Consalez G, Grassi F. Epithelial V-like antigen (EVA), a novel member of the immunoglobulin superfamily, expressed

in embryonic epithelia with a potential role as homotypic adhesion molecule in thymus histogenesis. J Cell Biol 1998;141:1061–71. [PubMed: 9585423]

7. DeMonte L, Porcellini S, Tafi E, Sheridan J, Gordon J, Depreter M, Blair N, Panigada M, Sanvito F, Merati B, Albientz A, Barthlott T, Ozmen L, Blackburn C, Guttinger M. EVA regulates thymic stromal organisation and early thymocyte development. Biochem Biophys Res Commun 2007;356:334–40. [PubMed: 17362876]
8. Carrithers M, Tandon S, Canosa S, Michaud M, Graesser D, Madri J. Enhanced susceptiablility to endotoxic shock and impaired STAT3 signaling in CD31-deficient mice. American Journal of Pathology 2005:11.
9. Carrithers M, Dib-Hajj S, Carrithers L, Tokmoulina G, Pypaert M, Jonas E, Waxman S. Expression of the voltage-gated sodium channel NaV1.5 in the macrophage late endosome regulates endosomal acidification. J Immunol 2007;178:7822–32. [PubMed: 17548620]
10. Data accessible at http://arrayconsortium.tgen.org/np2/searchForProjects.do?criteria.propo.
11. Pokutta S, Herrenknecht K, Kemler R, Engel J. Conformational changes of the recombinant extracellular domain of E-cadherin upon calcium binding. Eur J Biochem 1994;223:1019–26. [PubMed: 8055942]
12. Guo X, Rao JN, Liu L, Turner DJB, Barbara L, Wang J-Y. Regulation of adherens junctions and epithelial paracellular permeablility: a novel function for polyamines. Am J Physiol Cell Physiol 2003;285:5.
13. Ko K, Arora P, Bhide V, Chen A, McCulloch C. Cell-cell adhesion in human fibroblasts requires calcium signaling. J Cell Sci 2001;114:1155–67. [PubMed: 11228159]
14. D'Souza-Schorey C. Disassembling adherens junctions: breaking up is hard to do. Trends Cell Biol 2005;15:19–26. [PubMed: 15653074]
15. Pelosini M, Focosi D, Rita F, Galimberti S, Caracciolo F, Benedetti E, Papineschi F, Petrini M. Progressive multifocal leukoencephalopathy: report of three cases in HIV-negative hematological patients and review of literature. Ann Hematol 2008;87:405–12. [PubMed: 18064459]
16. Berger J. Progressive multifocal leukoencephalopathy. Curr Neurol Neurosci Rep 2007;7:461–9. [PubMed: 17999891]
17. Kleinschmidt-DeMasters B, Tyler K. Progressive multifocal leukoencephalopathy complicating treatment with natalizumab and interferon beta-1a for multiple sclerosis. N Engl J Med 2005;353:369–74. [PubMed: 15947079]
18. Langer-Gould A, Atlas S, Green A, Bollen A, Pelletier D. Progressive multifocal leukoencephalopathy in a patient treated with natalizumab. N Engl J Med 2005;353:375–81. [PubMed: 15947078]
19. Van Assche G, Van Ranst M, Sciot R, Dubois B, Vermeire S, Noman M, Verbeeck J, Geboes K, Robberecht W, Rutgeerts P. Progressive multifocal leukoencephalopathy after natalizumab therapy for Crohn's disease. N Engl J Med 2005;353:362–8. [PubMed: 15947080]

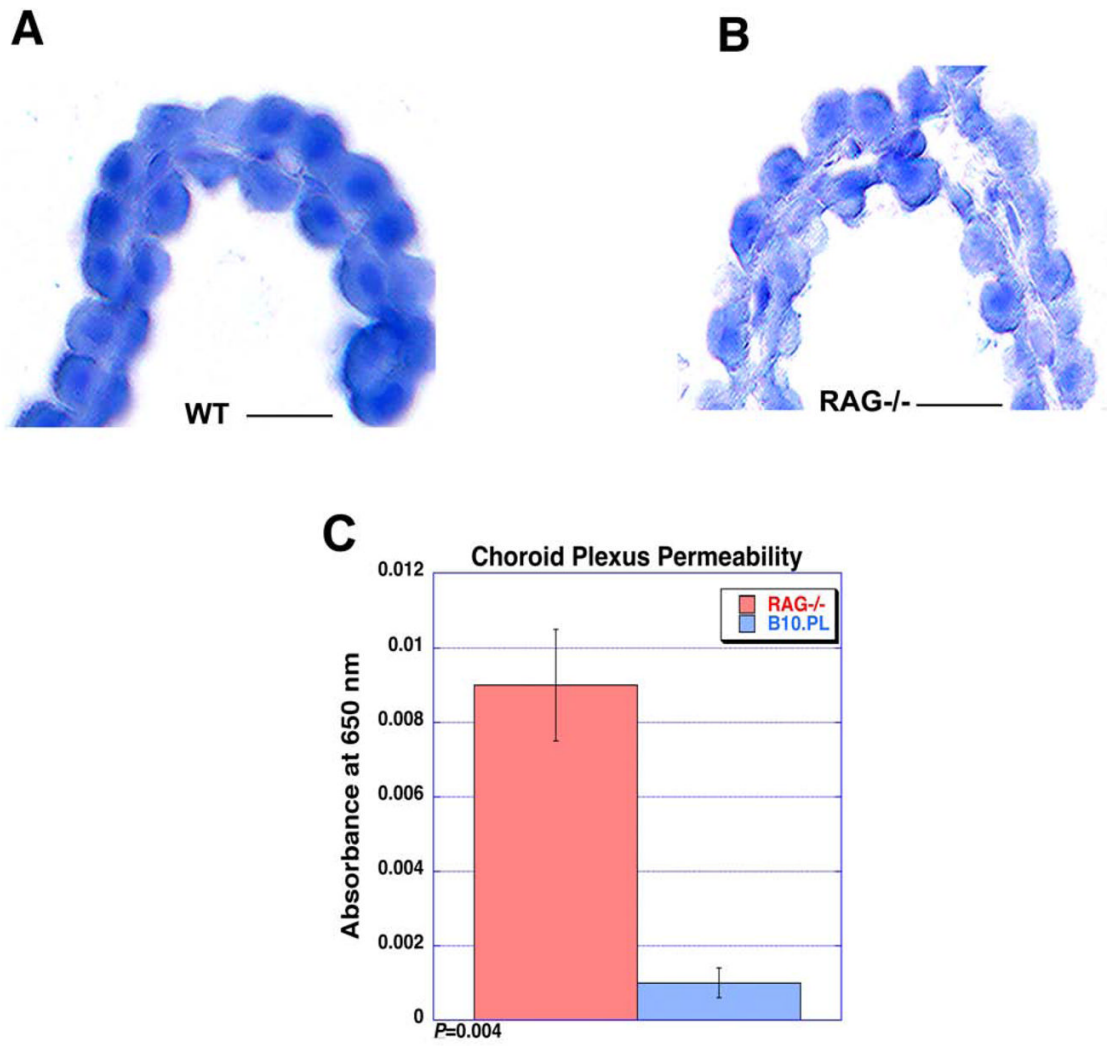

Figure 1. Altered choroid plexus morphology and increased permeability in lymphocyte deficient mice

(A–B) The choroid plexus in wild type C57BL6/J wild type (A) as compared to lymphocyte deficient RAG−/− mice (B) demonstrated distinct differences in morphology as determined by hematoxylin staining. The outer epithelial layer is more ordered and continuous in the wild type as compared to knockout animal (frozen section; hematoxylin). There was no evidence of any inflammatory infiltrate in either sample. (C) Permeability of microdissected choroid plexus was analyzed using the Evans Blue technique. Consistent with the altered morphology observed by histologic analysis, there was substantially greater linkage of intravascular Evans Blue dye into the choroid plexus structure in RAG−/− mice as compared to wild type controls. As normalized to tissue weight, the OD650 was 0.009 ± 0.0015 for RAG−/− and 0.001 ± 0.0004 for wild type (n=5; *P*=0.004). Scale bar, 20 μm.

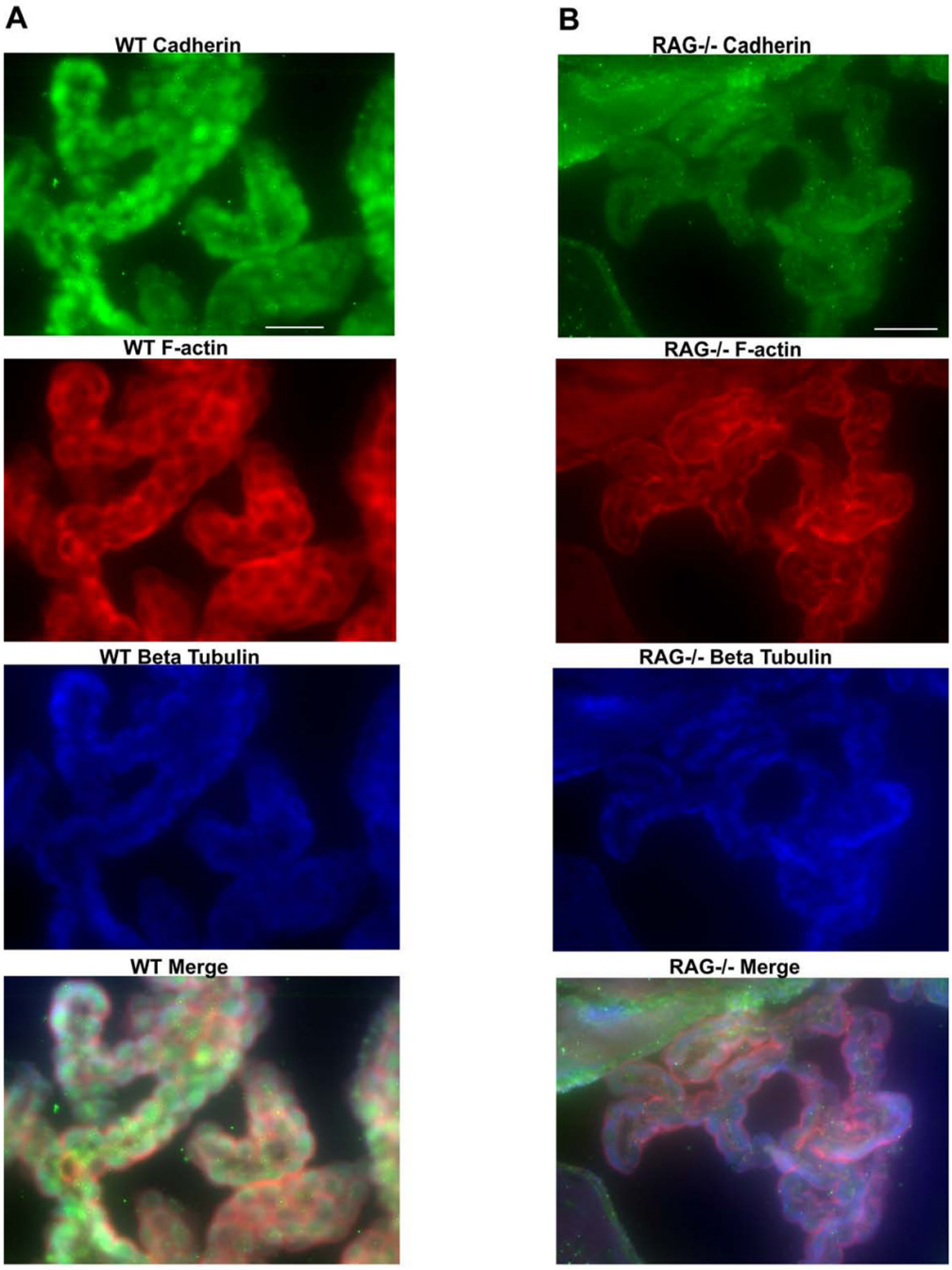

Figure 2. Decreased cadherin expression and altered F-actin localization in RAG−/−C57BL6/J mice as compared to wild type controls

(A–B) Brain sections from healthy, 6–8 week old wild type (A; left panels) and RAG−/− (B; right panels) mice were stained with primary anti-pan cadherin and microtubule-specific anti-α-tubulin antibodies, followed by fluorescent secondary antibodies and then phalloidin-Alexa 546 to label F-actin. As seen in Fig. 1, wild type choroid plexus demonstrated a more ordered, beaded appearance. Cadherin (green fluorescence; top panels) expression was much more intense in wild type mice as compared to lymphocyte deficient RAG−/− mice. In RAG−/− mice, there was positive cadherin staining along the ependymal cell border of the ventricle (upper left and upper center) but is near background levels in the choroid plexus. We also

observed an altered staining pattern for F-actin (red fluorescence) in RAG−/− mice as compared to wild type mice. In wild type mice, there was relatively intense staining at junctions between the choroid plexus epithelial cells that was not as apparent in RAG−/− mice. There was no evidence of a difference in staining intensity or localization in α-tubulin staining (blue fluorescence) between the two conditions. Scale bar, 40 μm.

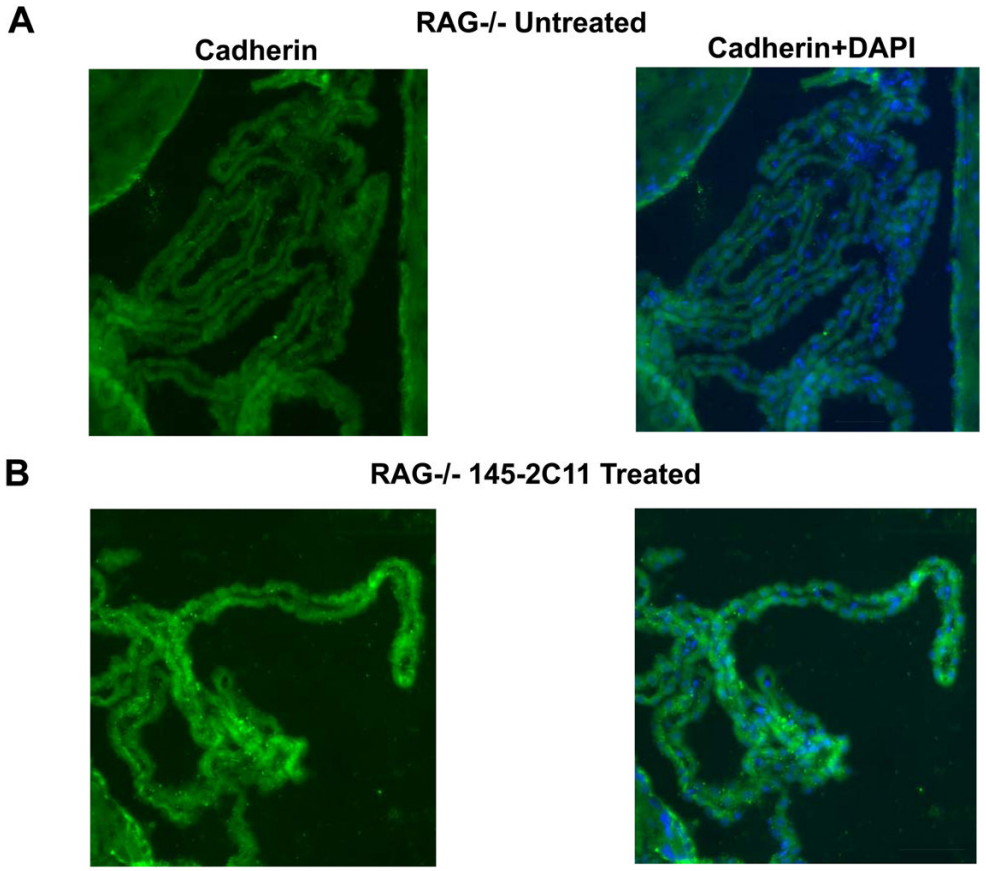

Condition	Densitometric Sum/Cell	No. of Cells Analyzed	n= (no. of mice/group)
RAG-/- Untreated	14 ± 5	200	3
RAG-/- 2C11	226 ± 52	215	6

P=0.01

Figure 3. Increased cadherin staining in RAG−/− choroid plexus following *in vivo* treatment with an EVA binding monoclonal antibody, 145-2C11

(A–B) Cadherin staining of choroid plexus was analyzed in untreated RAG−/− mice (A) and in those that were treated (B) with 145-2C11 24 hrs prior to sacrifice (50 μg iv). Treated mice demonstrated more intense staining for cadherin as compared to untreated mice. As shown in the Table below the micrographs, quantitative analysis of this staining revealed a statistically significant difference between the conditions. Scale bar, 40 μm.

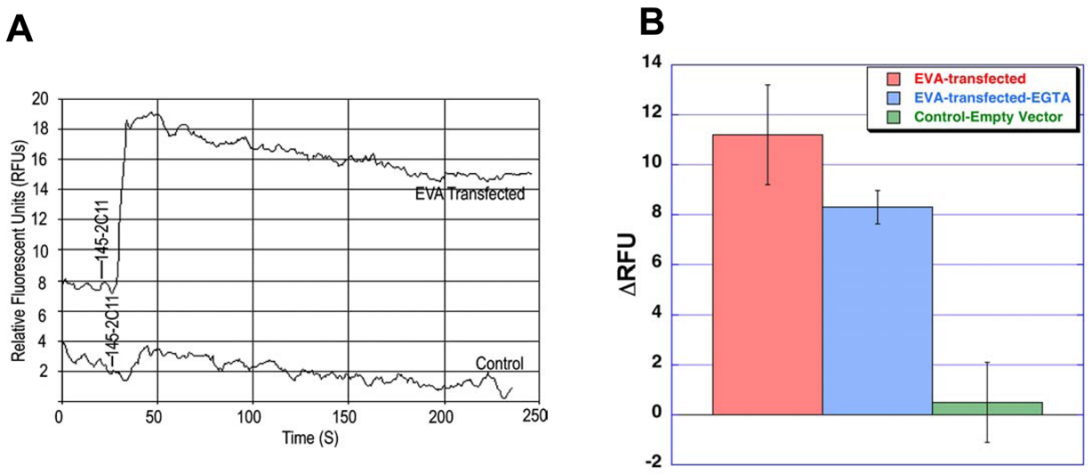

Figure 4. Calcium mobilization in HEK-293 cells transfected with mouse EVA-1 and challenged with 145-2C11

(A) HEK-293 cells were transfected with EVA-1 and analyzed for calcium responses to 145-2C11 in Fluo-4 loaded cells. Transfected cells (top curve) demonstrated a rapid and persistent increase in cytosolic calcium in response to 145-2C11 (0.5 μg/ml final concentration) that was not seen in control cells transfected with empty vector (bottom curve). Chelation of extracellular calcium with EGTA (4 mM) reduced the peak response, although this difference was not statistically significant (curve not shown). (B) Quantitative analysis of the peak changes demonstrated a statistically significant difference between the transfected and control conditions. For the EVA-transfected condition, the ΔRFU=11.2 ± 2.0 (n=5), for the untransfected condition ΔRFU=0.5 ± 1.0 (n=4) (P= 0.004 as compared to the transfected condition), and for the transfected condition with EGTA ΔRFU=8.3 ± 0.67 (n=3).

Table I

Real time PCR analysis of EVA and E-cadherin expression from microdissected choroid plexus.

Condition	EVA (Ct ± SEM)	n=	E-Cadherin (Ct ± SEM)	n=	GAPDH (Ct)
Wild Type Untreated	26.81 ± 0.35*	9	26.24 ± 0.13*	6	20.0
Wild Type 2C11	27.38 ± 0.20	6	27.02 ± 0.19	6	20.0
RAG−/− Untreated	29.55 ± 0.13	9	29.18 ± 0.03	6	20.0
RAG−/− 2C11	28.18 ± 0.20**	6	27.88 ± 0.06*	6	20.0

Real time PCR analysis was performed as described in Materials and Methods. Ct values were normalized using GAPDH expression as a control (Ct=20.0). For EVA expression, *P<0.0001 and **P=0.0003 as compared to the RAG−/− untreated condition. For cadherin expression, *P<0.0001 for both conditions as compared to the RAG−/− untreated condition. Ct: Threshold cycle.